Excited-state photoionization of Ce^{3+} ions in Ce^{3+}:CaF_2

G. J. Pogatshnik* and D. S. Hamilton

Department of Physics and Institute of Materials Science, University of Connecticut, Storrs, Connecticut 06268

(Received 5 June 1987)

The formation of stable color centers in Ce^{3+}:CaF_2 is found to result from the optical pumping of the lowest $4f \rightarrow 5d$ absorption band of the Ce^{3+} ions at C_{4v} symmetry sites with a 308-nm excimer laser. Absorption spectra of these color centers indicate that they are Ce^{2+} ions located at sites having O_h symmetry. The color centers are photochromic since they can be optically bleached. Measurements of the dependence of the number of photochromic color centers on the incident laser intensity and length of exposure are presented. The data is interpreted in terms of a two-step photoionization of the Ce^{3+} ions and the subsequent electron capture at a Ce^{3+} ion having O_h symmetry. Rate equations incorporating a two-photon creation term and a one-photon bleaching term are formulated and their solutions are consistent with the observed color-center growth kinetics. The implications of this work for other potential vibronic laser materials are also discussed.

I. INTRODUCTION

The spectrally broad vibronic emission bands in impurity-doped solids serve as the basis for wavelength-wavelength-tunable laser operation in these materials. But because of the broad emission and absorption bands, these materials are susceptible to excited-state absorption (ESA) which can significantly reduce the performance characteristics of the laser material. We have observed a strong ESA in Ce^{3+}:CaF_2 at the optical pumping wavelengths which lie in the near-ultraviolet (uv) region. It is a two-step process, where the first photon absorbed promotes an electron from the $4f$ ground state to the lowest $5d$ state of the trivalent cerium ion. Within the lifetime of this excited $5d$ state, a second photon is absorbed which then photoionizes the ion by promoting that electron to the conduction band. The free electron subsequently traps out at an electron acceptor site forming a stable color center. These color centers are absorptive at the wavelengths for stimulated emission of the trivalent cerium ions, and hence they serve as a quenching mechanism for laser gain in this crystal. The color centers produced are photochromic in that they can be optically bleached.

We have pursued the understanding of this two-step photoionization and color-center formation process in some detail, motivated by the facts: (a) that similar processes may occur in other lanthanide– or transition-metal-ion–doped solid-state laser materials which would operate in the deep-blue or near-ultraviolet region, (b) that the uv-induced discoloration is a prototypical laser damage process for which an impurity ion serves as a nucleation site, (c) that photochromic materials have significant potential in optical storage technologies, and (d) that Ce^{3+}:CaF_2 is a well-studied material and thus much of the background information concerning its optical properties is already in hand. In this work we will demonstrate that the properties of these laser-induced color centers can be explained by a model based on the excited-state photoionization (ESPI) of the cerium ions.

In Sec. II we will review the basic properties of the Ce^{3+}:CaF_2 system which will be of importance. Section III then examines the optical characteristics of the laser induced color center and the kinetics of its formation. A model based on simple rate equations for the ESPI process and the kinetics of the color center formation will be presented in Sec. IV followed by a summary of the results and implications of this work in Sec. V.

II. THE Ce^{3+}:CaF_2 SYSTEM

Calcium fluoride crystallizes in the fluorite structure. This structure consists of a cubic array of F^- ions with a divalent calcium ion situated at every other body center of the fluorine cubes. When cerium is incorporated into CaF_2 as an impurity ion, it enters in a trivalent state and substitutes for a calcium ion. The substitution of a Ce^{3+} ion for a Ca^{2+} ion requires the presence of an additional charge compensator to maintain the overall charge neutrality of the crystal. In crystals where the oxygen impurity content is low, the dominant charge compensation scheme is an additional F^- ion located in the nearest body-center cube position to the cerium impurity. This introduces a tetragonal distortion to the cubic symmetry at the impurity site so that the symmetry of the cerium ion is C_{4v}. In addition to the C_{4v} sites, there are also a few cerium ion sites which maintain their cubic symmetry.[1] These O_h symmetry sites occur when the F^- charge compensator is located further away from the trivalent cerium ion. As the distance between the cerium ion and the charge compensator increases, the strength of the tetragonal distortion of the crystal field at the cerium ion site is reduced. This restores the symmetry at the cerium site to O_h while maintaining overall charge neutrality in the crystal. The presence of cerium ions at sites of cubic symmetry is of great importance in this investigation, since cerium ions at these sites have previously been shown to be relatively stable in a divalent, as well as trivalent state. Thus, the trivalent ions at O_h sites can act as electron traps in the crystal.[2]

The optical absorption and fluorescence spectra of a Ce^{3+}:CaF_2 sample is shown in Fig. 1. The spectral features of this material have been previously investigated.[3,4] The broad absorption band centered at 310 nm corresponds to the lowest $4f \rightarrow 5d$ transition of the Ce^{3+} ion. The Ce^{3+} fluorescence is characterized by a 40-nsec radiative lifetime.

III. EXPERIMENTAL PROCEDURES AND RESULTS

The samples used in these experiments were grown by Optovac Inc. using a slow anneal Bridgman-Stockbarger method. The measurements were carried out with samples whose cerium ion concentration ranged from 0.001% to 1%. The majority of the measurements presented here were made using a 0.05% cerium-doped sample.

The lowest $4f \rightarrow 5d$ absorption band of the Ce^{3+} ions is resonant with the 308 nm output of a XeCl excimer laser. Illumination of the sample at this wavelength, using a Quanta Ray EXC-1 excimer laser, produces long-lived color centers in the material. The presence of these centers can be observed visually, with the sample changing from its original transparent state to a reddish-brown color. The mechanism responsible for this coloration is directly linked to the excitation of the cerium ions. Comparable flux illumination using the 337 nm output of a nitrogen laser, or the 355 nm output of the third harmonic of a Nd:YAG laser (where YAG denotes yttrium aluminum garnet), both of which are nonresonant with the cerium absorption bands, produces no coloration of the crystal. Similarly, no coloration of undoped CaF_2 is observed after exposure to the 308-nm laser light. Thus the coloration process must involve the cerium ion in the excited $5d$ level.

The centers that are responsible for this coloration are photochromic, in that the crystal can reversibly change color under optical illumination. That is, the Ce^{3+}:CaF_2 sample can be bleached back to the original transparent state by illumination of the sample at wavelengths which

are absorbed by the color centers. The bleaching process presumably takes place by a one-step photoionization transition on these centers.

The optical absorption spectrum of the color centers produced by the uv-laser irradiation at 308 nm is shown in Fig. 2. The spectrum was recorded using a Cary 14R spectrophotometer and the data is shown for both room temperature and liquid-nitrogen temperature. The spectral features of these color centers correspond to the optical properties of divalent cerium ions at O_h sites in CaF_2. The presence of Ce^{2+} in CaF_2 has been previously observed in both γ-irradiated crystals[2] and crystals treated by additive coloration.[5] The photochromic properties of divalent cerium in additively colored CaF_2 crystals have been well documented.[6-10] The additive coloration process in Ce:CaF_2 results in the formation of a composite color center consisting of an F' center (anion vacancy with two trapped electrons) on a $\langle 111 \rangle$ site next to a Ce^{3+} impurity ion. This composite center is sometimes referred to as an REF (rare-earth–F) center. The absorption spectrum of the additively colored crystals is dominated by the strong absorption bands of the REF center near 400 nm, which gives the crystal its green coloration. Illumination at wavelengths shorter than 400 nm partially bleaches the absorption bands of the REF center and produces divalent cerium ions with their concomitant absorption bands. Illumination into the divalent cerium absorption bands restores the REF bands to their original intensity. This photochromic process results from the transfer of an electron from the REF center through the conduction band, to a Ce^{3+} ion at a cubic site in the crystal. The electron transfer process can be summarized as

$$[REF] + Ce^{3+} \rightleftharpoons [REF]^+ + Ce^{2+} , \tag{1}$$
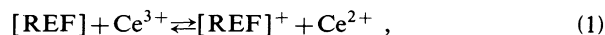
where the direction of transfer depends on the wavelength of light used for illumination of the sample. In these additively colored cerium-doped CaF_2 crystals, the
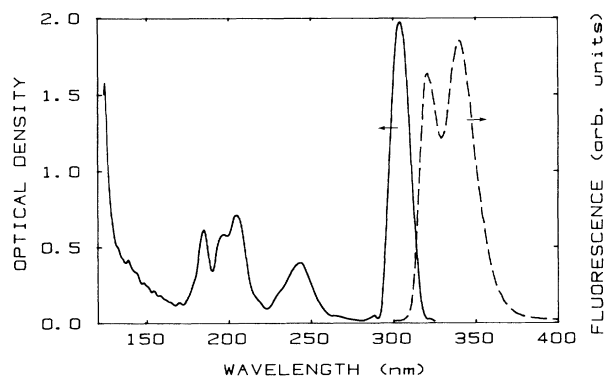
FIG. 1. Room-temperature optical absorption spectrum of 0.005% Ce^{3+}:CaF_2 (after Ref. 3) and the fluorescence spectrum following low-intensity 308-nm excitation.
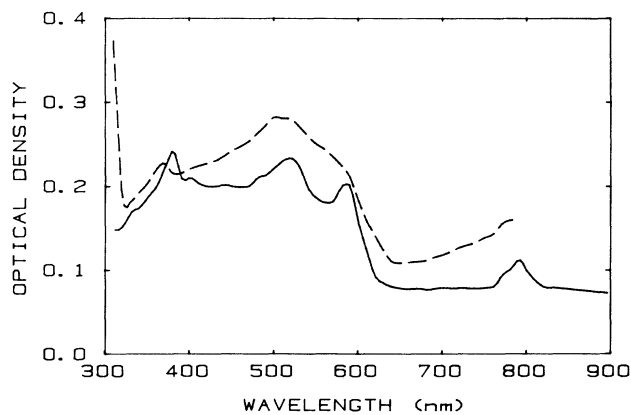
FIG. 2. Absorption spectra of the photochromic color center produced by the uv laser irradiation at 308 nm. Spectra are shown at 300 K (dashed curve) and 80 K (solid curve). The absorption bands are identified as those of divalent cerium.

excited electronic states for both the REF center and the Ce^{2+} lie near enough to the conduction band so that the electron transfer can occur in a single-photon transition.

We have observed a related process when the $Ce^{3+}:CaF_2$ crystals are pumped by the excimer laser, but in this case the photoionization of the Ce^{3+} ion does not occur in a one-photon absorption process. The absorption spectrum for $Ce^{3+}:CaF_2$ shows that the absorption band for the lowest $4f \rightarrow 5d$ transition lies well below the conduction-band transition. Therefore, one expects that the absorption of a 308-nm photon results in a purely localized transition at the cerium site. Nevertheless, intense laser pumping of the $Ce^{3+}:CaF_2$ sample at 308 nm does lead to a strong photoconductivity signal.[11] This suggests that a multiphoton process involving the Ce^{3+} ions is required for the photoionization of the trivalent cerium ions and the subsequent production of the divalent cerium centers.

The determination of the production mechanism for the formation of these divalent cerium centers is complicated by their photochromic nature. That is, the near-uv laser illumination responsible for the formation of these centers also causes them to bleach. Two simple experiments demonstrate this effect. Initially the 308-nm laser light is focused onto a 4-mm^2 area of the sample. The laser is run at a 10-Hz repetition rate with an output energy of approximately 10 mJ/pulse. After a few seconds, the illuminated region is darkened due to the formation of divalent cerium centers. The sample is then translated to an uncolored region and the irradiation is repeated. The newly irradiated area begins to darken but the previously irradiated area begins to bleach. The optical excitation of the sample produces a strong uv fluorescence from the radiative relaxation of the Ce^{3+} ions. The light from this luminescence is absorbed by the divalent cerium ions and causes them to bleach. It is also possible to observe this bleaching process without translating the sample. After the sample is colored by illumination with the excimer laser, the laser intensity was reduced. Continued illumination at the lower laser intensity then reduces the coloration, with the sample eventually becoming quite transparent. Both the Ce^{3+} fluorescence and the 308-nm light are absorbed by the divalent cerium centers and thus can bleach the color-center population. From these observations we can infer that a model which describes the appearance of divalent cerium ions following laser excitation, must account for a nonlinear creation process and the simultaneous optical bleaching of these centers. At a given laser intensity, these two competing processes will reach a dynamic equilibrium at a particular density of divalent cerium ions.

To determine in more detail the processes responsible for coloration of the crystal following uv excitation, we have measured the absorption produced by the presence of Ce^{2+} ions as a function of laser intensity and elapsed exposure time. A diagram of the experimental apparatus is shown in Fig. 3. The pump beam generated by the excimer laser passed through a 1-cm-diam circular aperture in order to assure relative spatial uniformity of the beam profile. The pump light was then focused to
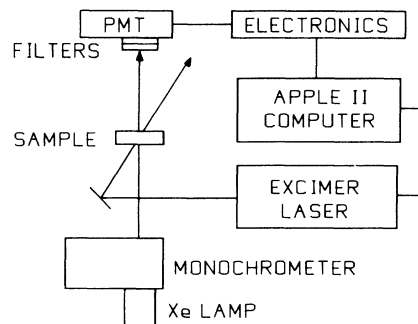
FIG. 3. Experimental apparatus used to investigate the spectral and growth characteristics of the color centers. The electronics used to interface the photomultiplier tube to the microcomputer include a current-to-voltage converter, a gated integrator, and a 12 bit analog-to-digital converter.

a 3-mm^2 spot onto a 2-mm-thick 0.05% $Ce^{3+}:CaF_2$ sample at room temperature. The intensity of this beam was varied by inserting metallic-coated neutral-density filters, whose transmission was calibrated at the 308-nm wavelength of the laser emission. The probe beam was generated by a 75-W xenon lamp focused onto the entrance slit of a $\frac{1}{4}$m Jarrell Ash monochromator. The monochromator was tuned to match the 520-nm absorption peak of the divalent cerium ions. The intensity of the probe beam was attenuated in order to minimize the effects of bleaching by the probe light. The probe beam was collimated and focused onto the sample to a 1-mm-diam spotsize which was concentric with the region illuminated by the pump beam. An alternate source for the probe beam was a 633-nm He-Ne laser whose output could be more tightly focused than that from the xenon lamp. A series of filters was used to block the uv fluorescence of the cerium ions and the scattered pump light from reaching the probe-beam detector. The intensity of the transmitted probe beam was measured using a Hamamatsu R928 photomultiplier tube. The resulting signal was averaged using a Stanford Research Systems model 250 gated integrator and then read by a 12 bit analog-to-digital converter card interfaced to an Apple II microcomputer.

The intensity of the transmitted probe beam was measured at a fixed 308-nm laser flux for a series of incident laser pulses. The resulting change in the optical absorption produced by the creation of divalent cerium centers was then calculated. Typical data curves for the uv laser-induced absorption as a function of the number of laser pulses for a series of different incident laser intensities are illustrated in Fig. 4. At a given laser intensity, the absorption of the 520-nm probe beam due to the Ce^{2+} centers increases for the first few laser pulses and then eventually reaches a steady-state level. The magnitude of this steady-state absorption is a function of the incident laser intensity as shown in Fig. 5. For low laser intensities the value of the steady-state absorption coefficient is almost linearly dependent on the incident laser intensity. As the intensity of the 308-nm laser increases, the value of the steady-state absorption
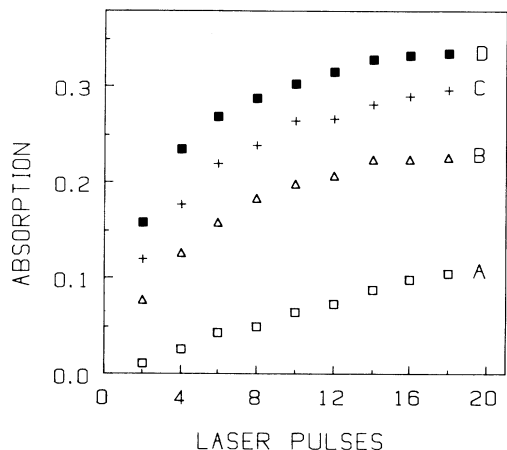
FIG. 4. The absorption $(\ln I_0 / I)$ of a 520-nm probe beam due to the growth of the divalent cerium color centers with accumulated exposure to the pulsed 308-nm laser. The laser intensities in MW/cm^2 are A, 10; B, 23; C, 33; D, 44.

coefficient begins to saturate, and finally becomes fixed at a value which is independent of laser intensity.

This saturation of the steady-state density of divalent cerium ions at high laser intensities indicates that there is an upper bound on the number of these centers which can be produced. The magnitude of the steady-state absorption coefficient depends on the laser intensity and the cerium concentration in the sample, but is independent of the initial concentration of Ce^{2+} ions. For example, illuminating the sample at high laser intensities produces a relatively dark crystal. If the intensity of the laser is now decreased and the illumination continued, the optical density of the sample will be reduced until it again reaches a steady-state value. The density of Ce^{2+} centers created in this process is the same as one would have obtained through illumination of an originally
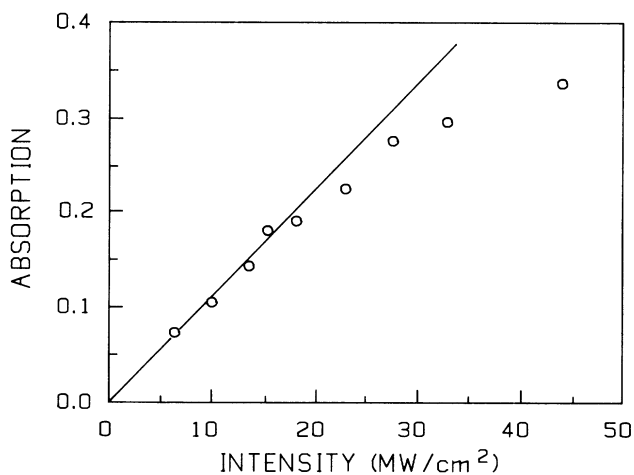
FIG. 5. Steady-state absorption $(\ln I_0 / I)$ at 520 nm due to presence of the divalent cerium color centers as a function of the peak intensity of the 308-nm laser. The straight line represents the linear approximation of Eq. (12).

transparent sample at the lower laser intensity. This behavior indicates the nonlinear nature of this process. If both the creation rate and bleaching rate for producing the divalent cerium centers were linearly dependent on the incident laser intensity, additional exposure to the reduced intensity laser light could not account for the decrease in the steady-state optical absorption of the sample.

The steady-state absorption in these samples reflects an equilibrium between the creation of the divalent cerium centers and their optical bleaching at a particular value of the laser intensity. To determine how the creation of the centers depends on the incident laser intensity, we have examined the slope of the absorption curves of Fig. 4 in the limit as the number of laser pulse exposures goes to zero. The extrapolation to the initial slope should be an accurate reflection of the creation process, since the competing bleaching term will depend on the initial concentration of Ce^{2+} centers. Initially, this concentration is approximately zero, so that the bleaching effects can be ignored. To determine the initial slope, the data from Fig. 4 were fit to the functional form $A = A_0(1 - e^{-\phi N})$ using a least-squares technique. Here A_0 is the steady-state absorption value, ϕ is the rate coefficient, and N is the number of laser pulses. The slope was taken by evaluating the derivative of the function in the limit $N \to 0$. Figure 6 shows the initial slope of the induced absorption from this analysis as a function of laser intensity. At low laser intensities, the log-log plot is nearly linear with a slope of 2. This indicates that the creation process for the divalent cerium centers depends on the square of the 308-nm intensity and thus two photons are required to photoionize the Ce^{3+} ions. At higher intensities, the dependence of the initial slope on the laser intensity begins to roll off and eventually becomes quasilinear. The data available in previous reports[12,13] concerning this behavior were limited to the high-flux region and thus were misinterpreted as indicating a one-photon ionization of the Ce^{3+} ions. We now understand this linear region as a breakdown of the $N \to 0$ limit at high-intensity illumination. That is, for sufficiently high laser flux, bleaching and saturation effects cannot be ignored even during the first laser pulse.
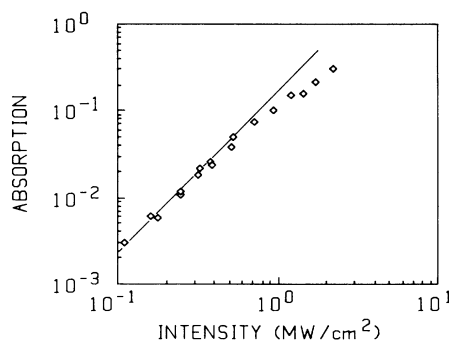
FIG. 6. Initial value of the change per laser pulse in the absorption of the 520-nm probe beam. The values for the lower intensity points depend quadratically on the laser intensity, as indicated by the straight line of slope 2.

IV. ANALYSIS AND DISCUSSION

The results of our measurements identify the divalent cerium ions at cubic sites in the crystal as those responsible for the coloration and also leads to a model which explains the kinetics of their formation. The model is based on a rate equation for the number of divalent cerium centers as a function of time (number of laser pulses), and incident laser flux. The model must incorporate several essential features. It must reflect the fact that the Ce^{2+} ions result from the optical excitation of the Ce^{3+} ions in a nonlinear process. Presumably, this entails raising an electron from the $4f$ ground state of the cerium ion to the conduction band via the $5d$ excited state. The model must also explain the photochromatic properties of the system. This involves the trapping of electrons at Ce^{3+} ions with O_h symmetry, thus forming Ce^{2+} ions, and the reverse photobleaching process of these centers. Finally, the model must account for the observed steady-state limit for the density of divalent cerium ions as a function of laser intensity. For low intensities, the steady-state absorption coefficient increases with intensity. As the intensity is increased however, density of Ce^{2+} ions tends to saturate at a value which is flux independent.

The appearance of divalent cerium is initiated through the photoionization of Ce^{3+} ions, which are predominantly at C_{4v} sites in the CaF_2 crystal. This photoionization process occurs by an ESA transition from the excited $5d$ state of the Ce^{3+} ion. Ignoring the electron transfer which follows the photoionization, this two-step ESA will involve the number of cerium ions at the C_{4v} sites which are in the $4f$ ground state (n_{4f}), in the excited $5d$ state (n_{5d}), and those whose electron has been promoted to the conduction band and thus photoionized (n_{PI}). The rate equations which describe the ESPI process are

$$dn_{4f}/dt = -n_{4f}\sigma F \ ,$$
$$dn_{5d}/dt = n_{4f}\sigma F - n_{5d}\sigma^* F \ , \qquad (2)$$
$$dn_{PI}/dt = n_{5d}\sigma^* F \ ,$$

where σ is the $4f \rightarrow 5d$ cross section, σ^* is the excited-state absorption cross section from the $5d$ state to the conduction band, and F is the incident laser flux in photons $cm^{-2} sec^{-1}$. We have assumed for these rate equations that the laser pulse width Δt is much less than the lifetime of the cerium $5d$ excited state, so that the excited-state density does not appreciably decay during the time when the radiation field is present. For our measurements in $Ce^{3+}:CaF_2$, $\Delta t \approx 5$ ns, which is nearly an order of magnitude shorter than the 40-ns fluorescence decay time of the lowest $5d$ level. We will also assume that $n_{4f} + n_{5d} + n_{PI} = n_t$, where n_t is the approximately constant number of cerium ions with tetragonal C_{4v} symmetry.

For a rectangular laser pulse of a duration Δt, these rate equations can be solved for the number of cerium ions which are photoionized by each laser pulse,

$$n_{PI} = \frac{n_t}{\sigma - \sigma^*}[\sigma(1 - e^{-\sigma^* F\Delta t}) - \sigma^*(1 - e^{-\sigma F\Delta t})] \ . \quad (3)$$

This expression can be simplified considerably if the 308-nm laser pulse does not saturate either transition. Thus with the assumption that $\sigma^* F\Delta t \ll 1$ and $\sigma F\Delta t \ll 1$, Eq. (3) becomes

$$n_{PI} = n_t \sigma \sigma^* F^2 \Delta t^2 / 2 \ . \qquad (4)$$

The solution leads to an equivalent single rate equation for the number of cerium ions photoionized per pulse as

$$dn_{PI}/dt = n_t \sigma \sigma^* F^2 \Delta t \ . \qquad (5)$$

Within the limitations noted above, the ESPI process depends quadratically on the laser flux and on the product of the two relevant cross sections, σ and σ^*.

Once the original photoionization process is understood, the electron trapping and photochromic nature of this system is analogous to that in additively colored $Ce^{3+}:CaF_2$ crystals. In our measurements, the electrons are released through a two-step excited-state photoionization of the Ce^{3+} ions instead of the one-photon ionization of the REF center. Trivalent cerium ions at cubic sites in the crystal act as trap sites for these electrons. Since the charge compensator at these O_h symmetry sites is somewhat removed from the cerium impurity, the Ce^{3+} ions at these sites will have a net positive local charge associated with their lattice position. The Coulombic field produced by these ions provides a net attractive potential for electrons in the conduction band which causes them to trap at these sites. This trapping results in the formation of divalent cerium ions at the cubic sites and accounts for the coloration of the crystal. Subsequent illumination into the Ce^{2+} absorption bands ionizes these centers, and returns some of the electrons to the originally ionized sites. This restores the valence state of all the cerium ions to trivalent and accounts for the photochromic behavior of this material.

The flux dependence of the steady-state absorption coefficient due to the divalent cerium centers reflects the competition between the creation and bleaching of these centers. Since the bleaching term is linear in intensity and the creation term is nonlinear, the equilibrium value of the divalent cerium ion density will be dependent on the incident laser intensity.

A model can now be established for the formation of divalent cerium centers in optically pumped $Ce^{3+}:CaF_2$. We shall first define the relevant parameters for the development of a rate equation for the number of divalent cerium color centers. The density of Ce^{3+} ions at tetragonal sites is n_t. These are the ions excited by the 308-nm laser light and are subject to photoionization. The density of Ce^{3+} ions at cubic sites is n_c which are the unfilled electron trap sites, and n_d, the density of divalent cerium ions, represents the cerium ions at cubic sites which have changed valence by trapping an electron. The parameters n_c and n_d are constrained by the relation

$$n_c + n_d = n_{c0} \ , \qquad (6)$$

where n_{c0} is the density of Ce^{3+} ions at cubic sites which are initially present in the crystal.

The rate equation for the formation of divalent cerium

centers due to the laser excitation is then given by

$$dn_d/dt = n_t n_c \alpha F^2 - n_d \beta F \ . \tag{7}$$

The first term in Eq. (7) represents the creation of the divalent cerium ions due to the ESPI and the subsequent electron trapping. It depends on the product of the number of Ce^{3+} ions available for photoionization and the number of available trap sites. It also depends on the square of the incident laser flux, F, and on a parameter α, where α is the product of the $4f \rightarrow 5d$ absorption cross section σ, the excited-state photoionization cross section σ^*, and an electron-capture cross section at the trap sites. The second term represents the bleaching of the divalent cerium centers by both the fluorescence photons from the $5d \rightarrow 4f$ spontaneous emission and the incident 308-nm photons. This term is equal to the product of the number of divalent cerium centers, the laser flux, and a bleaching cross section β. We will assume that n_t remains constant, which is justified by the large number of tetragonal ions compared to the number at cubic symmetry sites.

Equation (7) can be written in a more informative manner by using the relation $n_d + n_c = n_{c0}$. The rate equation then becomes

$$dn_d/dt = n_t(n_{c0} - n_d)\alpha F^2 - n_d \beta F \ . \tag{8}$$

We can examine this equation in the $t \rightarrow 0$ limit where $n_d \approx 0$. The initial rate for production of the divalent cerium centers is then

$$dn_d/dt \approx n_t n_{c0} \alpha F^2 \quad (t \rightarrow 0 \text{ limit}) \ . \tag{9}$$

This equation has the quadratic flux dependence that was shown in the initial absorption measurements of Fig. 6. However, at high values of the flux, there may be a significant number of divalent ions created in the first laser pulse as well as the possible onset of saturation effects. In this case, the initial slope of the data will have a somewhat lower flux dependence.

The steady-state solutions to Eq. (8) can be examined by setting $dn_d/dt = 0$, or

$$n_t(n_{c0} - n_d)\alpha F = n_d \beta \ . \tag{10}$$

This can be solved for the number of divalent cerium ion color centers as

$$n_d = \frac{n_t n_{c0} \alpha F}{n_t \alpha F + \beta} \ . \tag{11}$$

In the low-flux limit, $\beta \gg n_t \alpha F$, so that

$$n_d = \frac{n_t n_{c0} \alpha}{\beta} F \ . \tag{12}$$

Equation (12) shows that the steady-state absorption coefficient increases linearly with the laser flux for low intensities, in agreement with the experimental results displayed in Fig. 5. For high intensities, $n_t \alpha F \gg \beta$, so that,

$$n_d = n_{c0} \ . \tag{13}$$

This limit corresponds to the case where all of the available electron traps are filled. The steady-state absorption coefficient is then independent of the incident laser intensity. The saturation of the steady-state absorption with increasing laser flux in Fig. 5 reflects this limit.

This model is somewhat of a simplification in several respects. In particular, it is not only the purely C_{4v} cerium sites that are photoionized. A distribution of sites for the F^- charge compensator should lead to a set of absorption bands for the lowest $4f \rightarrow 5d$ transition which overlap at room temperature. Thus several types of cerium sites with symmetries differing from purely tetragonal may be photoionized by the incident laser field. However, since the predominant symmetry for the Ce^{3+} ions is C_{4v}, we expect that this effect is of minor consequence. Similarly, one does not expect that the photoionized electrons get trapped only on cerium ions at O_h sites. However, these cubic sites should preferentially trap the ionized electrons and remain stable for a longer period of time. Thus, the cerium ions at cubic sites are those responsible for the stable coloration of the crystal. A similar electron trapping situation occurs in $Gd^{3+}:CaF_2$ following exposure to x-ray irradiation.[14] This material also exhibits a photochromic effect similar to additively colored $Ce^{3+}:CaF_2$. Following x-ray irradiation there exists a long-term phosphorescence of the Gd^{2+} impurity ions as they thermally ionize. The spectral features of the emission change as a function of time following irradiation. The Gd^{2+} sites with lower symmetry decay the fastest, and after a sufficient length of time, the emission spectrum is dominated by Gd^{2+} ions at cubic sites. Aside from these caveats, our model accounts for all of the features of the coloration process in $Ce^{3+}:CaF_2$ following the laser excitation of the Ce^{3+} ions and accurately reproduces the quantitative experimental results.

Finally, one would like to use this model to determine the cross section for excited-state photoionization. Unfortunately this parameter cannot be determined from monitoring the absorption of the divalent cerium ions. As previously pointed out, the positive contribution to the creation rate contains a parameter α, which is the product of the $4f \rightarrow 5d$ cross section, the excited-state photoionization cross section, and a capture cross section for the electron at an alternate cerium site. This capture cross section reflects the branching ratio between the fraction of electrons which trap to form Ce^{2+} ions, and those which retrap on the originally ionized center. Since this branching ratio cannot be determined from the divalent cerium ion concentration, alternate methods are needed in order to obtain a numerical value for σ^*.

V. SUMMARY

Figure 7 illustrates the essential features of the model for ESPI in $Ce^{3+}:CaF_2$. Laser excitation of the lowest $4f \rightarrow 5d$ transition results in the photoionization of the Ce^{3+} ion through the $5d$ state. The electron is promoted to the CaF_2 conduction band where it has sufficient mobility to be trapped at an alternate trivalent cerium

Conduction Band
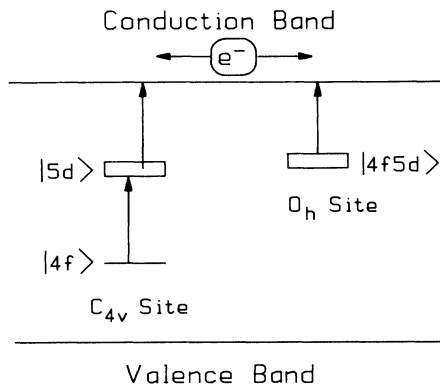
FIG. 7. Proposed model for the creation and bleaching of the photochromic center in Ce^{3+}:CaF_2.

site with cubic symmetry and thus form a divalent cerium center. These centers may be optically bleached by illumination into the Ce^{2+} absorption bands. This bleaching reverses the photochromic transition and returns the crystal to its original transparent state. A rate equation for the density of divalent cerium centers using this model accurately reproduces the experimental results.

In Ce^{3+}:CaF_2, the electron trap sites which are responsible for the coloration of the crystal, do not involve parasitic impurities or defects in the crystal, but result from alternate metastable valence states of the cerium ion. Our work demonstrates that systems which incorporate laser active centers which can exist in more than one valence state, and which are subject to excited state photoionization, may experience a degradation in laser performance due to the formation of this type of color center. While the extreme stability of Ce^{2+} in CaF_2 may be exceptional, it is not unreasonable to assume that this process may occur in other laser materials as well. The photoelectrons which result from the photoionization of a laser active ion may also trap at alternate lattice sites; however, the retrapping time may be on much shorter time scales than the many hours of the Ce^{3+}:CaF_2 system. Recent measurements of the single pass gain at 325 nm in Ce^{3+}:$YLiF_4$ indicate that both transient and stable color centers can be produced by ESPI from the pump radiation.[15] The stable color centers in this material result from fluorine vacancies which can trap an electron from the cerium photoionization. In addition to photoionization occurring by the excited-state absorption of a pump photon, it is also possible for a photon emitted during a fluorescence transition to be absorbed by another ion in its excited state and result in a photoionization process. Such a photoionization process occurs[13,16] in Ce^{3+}:$Y_3Al_5O_{12}$, where the excited-state absorption is strong enough to completely quench the gain due to stimulated emission.

Our observation that the Ce^{3+} ions at O_h symmetry sites in CaF_2 are efficient electron acceptors suggests that other rare-earth ions in related host materials should also play a similar role. The recent measurements of photon-gated hole burning[17] in Sm^{2+}:$BaClF$ indicate that Sm^{3+} serves as an effective electron trap site for the electrons released following the photoionization of the Sm^{2+} ions. For these measurements, two laser beams at different frequencies were used to photoionize the impurity ion via an excited-state absorption process. In Ce^{3+}:CaF_2, the two-step photoionization utilizes a single laser frequency to both excite the ion and then photoionize it. Similar single beam processes for other impurity ions may play an important role in frequency-domain optical storage devices.

ACKNOWLEDGMENTS

*Present address: Oak Ridge National Laboratories, Solid State Division, Oak Ridge, TN 37831.

[1] M. J. Weber and R. W. Bierig, Phys. Rev. 134, 1492 (1964).

[2] D. S. McClure and Z. J. Kiss, J. Chem. Phys. 39, 3251 (1963).

[3] E. Loh, Phys. Rev. 154, 270 (1967).

[4] W. J. Manthey, Phys. Rev. B 8, 4086 (1973).

[5] R. C. Alig, Z. J. Kiss, J. P. Brown, and D. S. McClure, Phys. Rev. 186, 276 (1969).

[6] D. L. Staebler, S. E. Schnatterly, and W. Zernik, IEEE J. Quantum Electron. QE-4, 575 (1968).

[7] D. L. Staebler and S. E. Schnatterly, Phys. Rev. B 3, 516 (1971).

[8] C. H. Anderson and E. S. Sabisky, Phys. Rev. B 3, 527 (1971).

[9] R. C. Alig, Phys. Rev. B 3, 536 (1971).

[10] R. Aldous and J. M. Baker, J. Phys. C 10, 4821 (1977).

[11] G. J. Pogatshnik, Ph.D. thesis, University of Connecticut, 1986.

[12] G. J. Pogatshnik, S. K. Gayen, and D. S. Hamilton, J. Lumin. 31/32, 250 (1984).

[13] D. S. Hamilton, in Tunable Solid State Lasers, edited by P. Hammerling (Springer-Verlag, Berlin, 1985), pp. 80–90.

[14] J. Makovsky, Phys. Rev. Lett. 15, 953 (1965).

[15] Ki-Soo Lim, Ph.D. thesis, University of Connecticut, 1986.

[16] D. S. Hamilton, S. K. Gayen, G. J. Pogatshnik, R. D. Ghen, and W. J. Miniscalco (unpublished).

[17] A. Winnacker, R. M. Shelby, and R. M. Macfarlane, Opt. Lett. 10, 350 (1985).